Acta Biochim Biophys Sin, 2020, 52(11), 1265–1273
doi:10.1093/abbs/gmaa124
Advance Access Publication Date: 20 November 2020
Original Article

Original Article

Preparation, characterization, and evaluation of antioxidant activity and bioavailability of a self-nanoemulsifying drug delivery system (SNEDDS) for buckwheat flavonoids

Zhijuan Zhao[1,2], Xiaodong Cui[1], Xiaoli Ma[1], and Zhuanhua Wang[1,*]

[1]Key Laboratory of Chemical Biology and Molecular Engineering of Ministry of Education, Institute of Biotechnology, Shanxi University, Taiyuan 030006, China, and [2]School of Pharmacy, Shanxi Medical University, Taiyuan 030001, China
*Correspondence address. Tel/Fax: +86-351-7011499; E-mail: zhwang@sxu.edu.cn

Received 27 April 2020; Editorial Decision 29 July 2020

Abstract

The self-nanoemulsifying drug delivery system has shown many advantages in drug delivery. In this study, a self-nanoemulsifying drug delivery system of buckwheat flavonoids was prepared for enhancing its antioxidant activity and oral bioavailability. A nanoemulsion of buckwheat flavonoids was developed and characterized, and its antioxidant, *in vitro* release, and *in vivo* bioavailability were determined. The nanoemulsion was optimized by the central composite design response surface experiment, and its particle size, polymer dispersity index (PDI), zeta potential, morphology, encapsulation efficiency, and stability were evaluated. The antioxidant activity was tested by measuring its 2,2-diphenyl-1-picrylhydrazyl scavenging activity, hydroxyl radical scavenging activity, and superoxide anion scavenging ability. *In vitro* release of buckwheat flavonoids nanoemulsion showed a higher cumulative release than the suspension, and the release fitting model followed the Ritger–Peppas and Weibull models. The effective concentration of the nanoemulsion was evaluated *in vivo* using a Wistar rat model, and the area under the plasma concentration-time curve of the buckwheat flavonoids nanoemulsion was 2.2-fold higher than that of the buckwheat flavonoid suspension. The C_{max} of the nanoemulsion was 2.6-fold greater than that of the suspension. These results indicate that the nanoemulsion is a promising oral drug delivery system that can improve the oral bioavailability to satisfy the clinical requirements.

Key words: buckwheat flavonoids, self-nanoemulsifying drug delivery system, nanoemulsion, antioxidant activity, bioavailability

Introduction

Buckwheat (genus: *Fagopyrum*; family: Polygonaceae), an important medicinal and edible herb, contains many bioactive compounds, including flavonoids, phenolic compounds, triterpenoids, amino acids, volatile compounds, etc. [1]. Buckwheat flavonoids contain a common benzo-g-pyrone structure and a polyphenolic structure consisting of a 15-carbon basic skeleton (C_6-C_3-C_6). The herb has various pharmacological activities, including antioxidant, anticancer, anti-inflammatory, and other activities [2–4]. Though buckwheat flavonoids possess diverse activities, their medicinal and edible values are limited due to the low solubility, low oral bioavailability, and poor systemic absorption. So, the clinical administration of buckwheat flavonoids requires a reasonably effective drug delivery system.

Recently, the self-nanoemulsifying drug delivery system (SNEDDS), a spontaneous emulsification method, has attracted increased attention [5–7], which can improve the oral bioavailability of hydrophobic drugs and bioactive food components [8]. The system is composed of various components, including oil phase, surfactant, cosurfactant, and water phase. The system has a variety of molding mechanisms, and the ultra-low or negative surface tension is considered as the main reason behind the formation of the nanoemulsion, and appropriate phase composition is important for the stability of nanoemulsion [9,10]. The diffusion of the

cosurfactant from the organic phase into the aqueous phase may also be an important mechanism for the formation of the nanoemulsion [11,12]. The small particle sizes in a drug delivery system offer many promising advantages, including smaller surface tension and greater stability. The smaller particle size offers a greater interfacial surface area for drug absorption, and the solubility and bioavailability are enhanced. For example, a SNEDDS of resveratrol with the droplet size of 50 nm exhibited better antioxidant capacity and less toxicity than free resveratrol [13]. SNEDDS of nintedanib (a poorly soluble molecule) significantly increased its area under the plasma concentration-time curve (AUC) [14]. Therefore, the self-nanoemulsifying drug delivery system can improve the bioactivity of encapsulated components, which can also potentially improve the medicinal and edible values of buckwheat flavonoid.

To enhance the antioxidant activity and oral bioavailability of buckwheat flavonoids, a SNEDDS of buckwheat flavonoids was prepared in this study. The preparation and optimization were based on the central composite design response surface experiment, and particle size, zeta potential, and encapsulation efficiency were determined. The study specifically focused on evaluating the antioxidant activity and comparing the oral bioavailability of the nanoemulsion with that of suspension *in vivo*.

Materials and Methods

Materials

Buckwheat flavonoids (purity >95%) were procured from Xi'an Tianxiang Bioengineering Co., Ltd (Xi'an, China). Rutin was purchased from the National Institute for the Control of the Pharmaceutical and Biological Products (Beijing, China). 2,2-Diphenyl-1-picrylhydrazyl (DPPH) was purchased from Phygene Life Sciences Co., Ltd (Fuzhou, China). The reagents used in high-performance liquid chromatography (HPLC) were chromatographically pure, and the other chemicals and reagents and solvents were of analytical grade.

Preparation and experimental design

Buckwheat flavonoids nanoemulsion was prepared through self-nanoemulsification. Briefly, PEG-40 hydrogenated castor oil (surfactant) and propylene glycol (cosurfactant) were thoroughly mixed with a magnetic stirrer at room temperature, and castor oil was added to the mixture. Subsequently, the buckwheat flavonoids were added into the admixture and stirred, until they were dissolved completely. Then, distilled water was added dropwise into the system until the nanoemulsion was formed.

The experimental design was carried out by the central composite design (CCD) response surface experiment [15, 16]. Based on the solubility study and the pseudo-ternary phase diagram, three factors of the oil phase (A), surfactant and cosurfactant (S_{mix}, B), and water phase (C) were used as the independent variables, and the particle size (Y_1) and encapsulation efficiency (Y_2) were considered as the dependent variables. Design-Expert 8.0.6 software was used to analyze the experimental data, and the three-dimensional response surface graphs were plotted. The fitted model was expressed by the coefficient of *R*, and its statistical significance was determined by the *F*-test.

Characterization of nanoemulsion

The particle size and zeta potential of the nanoemulsion were analyzed using the dynamic light scattering method with a Malvern Zetasizer (Malvern Instruments Ltd, Malvern, UK). The morphology of nanoemulsion was observed under a transmission electron microscope (JEM-1011; JEOL, Tokyo, Japan) at 200 kV accelerating voltage. Encapsulation efficiency was calculated using the formula: encapsulation (%) = $W_s/W_t \times 100\%$ (W_s and W_t are the amounts of the supernatant and total drug, respectively). The nanoemulsion was dispersed in methanol and then ultrasonicated at 37°C for 30 min. The mixture was centrifuged at 5000 *g* for 10 min, and the supernatant was analyzed by HPLC (Agilent 1200 LC; Agilent Tech Instrument Co, Santa Clara, USA) equipped with a C_{18} column (Agilent Zorbax, 250 mm×4.6 mm, 5 μm). A mixture of methanol and acetic acid (50:50) aqueous solution (0.5%) was used as the mobile phase at a flow rate of 1 ml/min. The stability of the nanoemulsion was tested at different temperatures (−40°C, 4°C, 25°C, and 37°C) for 30 days. The nanoemulsion was also examined for the phase separation by centrifuging at 3000 *g* and 10,000 *g*. The nanoemulsion was diluted 10- and 100-folds with distilled water to investigate the particle size, zeta potential, and stratification of the system.

DPPH scavenging activity The DPPH (0.2 mM, 1 ml) reagent was used for determining the antioxidant activity of the buckwheat flavonoid nanoemulsion (0.2, 0.4, 0.6, 0.8, and 1.0 mg/ml, 1 ml) [17, 18]. DPPH ethanol solution and nanoemulsion were mixed and kept in the dark for 30 min at room temperature, and the absorbance was measured at 517 nm. The mixtures of DPPH and distilled water were used as the controls. Meanwhile, the suspension and the ascorbic acid were also examined using the above method. The DPPH scavenging activity was calculated by the following equation:

$$\text{DPPH scavenging activity}\,(\%) = \frac{A_c - A_s}{A_c} \times 100\%$$

where A_s and A_c are the absorbance of sample and control, respectively.

Hydroxyl radical scavenging activity The hydroxyl radical scavenging activities of buckwheat flavonoid nanoemulsion and suspension and the ascorbic acid solution samples were measured as previously reported [19, 20]. In brief, $FeSO_4$ solution (2.5 mM, 1 ml) was added to the samples and then H_2O_2 (2.5 mM, 1 ml) and salicylic acid (2.5 mM, 1 ml) were added successively. The temperature of the mixture was adjusted to 37°C for 60 min. After completion of the reaction, the hydroxyl radical was measured by monitoring the absorbance at 510 nm. Meanwhile, distilled water in stead of the sample was used as the control. The scavenging activity of hydroxyl radicals was calculated with the following equation:

$$\text{Hydroxyl radical scavenging activity}\,(\%) = \frac{A_c - A_s}{A_c} \times 100\%$$

where A_s and A_c are the absorbance of sample and control, respectively.

Superoxide anion scavenging activity Pyrogallic acid (25 mM, 10 μl) was added to 3 ml of Tris-HCl buffer (pH 8.2). The absorbance of the mixture was determined every 30 s for 4 min at 325 nm. According to the absorbance, the auto-oxidation rate of pyrogallic acid was

evaluated by the slope of the absorbance-time curve. Then the samples (0.2, 0.4, 0.6, 0.8, and 1.0 mg/ml) were measured following the above method, and the scavenging rate of superoxide anion radical was calculated by the following formula [21]:

$$\text{Superoxide radicalscavenging activity}\,(\%) = \frac{V_c - V_s}{V_c} \times 100\%$$

where V_s and V_c are the scavenging rate of sample and control, respectively.

In vitro release experiment

In vitro release experiment was carried out by dynamic dialysis of nanoemulsion [22]. The nanoemulsion and suspension of buckwheat flavonoids were poured into activated dialysis bags (molecular weight cutoff, 8 kDa) and immersed in 50 ml of phosphate buffer saline (PBS; pH 7.4) at 37°C±0.5°C under continuous stirring at 100 rpm. Then, 2 ml of each sample was withdrawn at different time points (0.25, 0.5, 1, 2, 4, 8, 12, 24, 36, and 48 h), and an equal volume of PBS was replenished. The samples were examined by ultraviolet spectroscopy (UV 1200; Shanghai Meipuda Instrument Co., Shanghai, China) at 507 nm using $NaNO_2$-$Al(NO_3)_3$ colorimetric method, and the standard curve was A=0.0149C+0.1008 (r=0.9997). The cumulative release (Q) was calculated by the following formulas:

$$\text{Cumulative release}\,(\%) = \left(\frac{C_n V + V_i \sum_{i=1}^{n-1} C_i}{m}\right) \times 100\%$$

where C_i and C_n are the concentration at different time points, V and V_i are the volumes of 50 ml PBS and sample (2 ml), respectively, and m is the initial amount of drug (10 mg).

In vivo experiment

The Wistar rats (200±20 g) were obtained from the Experimental Animal Center of Shanxi Medical University (Taiyuan, China), and all experimental procedures were approved by the Institutional Animal Care and Use Committee of Shanxi Medical University. The animals were maintained under a 12/12 h light/dark cycle at 25±2°C and relative humidity of 60%±10%. The animals were provided free access to water and food (food was provided until 12 h before the experiment).

The buckwheat flavonoid nanoemulsion and suspension were administered intragastrically at a dose of 60 mg/kg to the test and control groups [23,24]. The blood samples (0.5 ml) were withdrawn from the fundus venous plexus into heparinized tubes at 0.083, 0.25, 0.5, 1, 2, 4, 8, 12, 24, and 48 h after oral administration of the drugs. The plasma was separated by centrifuging the blood sample at 10,000 *g* for 8 min. Then, the morin hydrate (internal standard) was added to 100 µl of plasma, vortexed for 3 min, and 300 µl of methanol was added subsequently and mixed for 5 min. The mixtures were centrifuged at 10,000 *g* for 8 min to precipitate the protein aggregates. The supernatant was dried, re-dissolved in 100 µl of methanol, and then centrifuged at 10,000 *g* for 5 min. The supernatants were analyzed by HPLC using a mobile phase containing methanol:acetic acid aqueous solution (0.5%; 50:50) at a flow rate of 1 ml/min. The analysis of samples and internal standard was not influenced by endogenous impurities. The standard curve, y=15,677 x+8.328 (r=0.9990), was plotted with the ratio of peak areas of the standard and internal standard as ordinate against the standard concentration as abscissa. The recovery rate was 95%–105%, and the relative standard deviation (RSD) was less than 3%; the RSD of precision was less than 3%, and the RSD of reproducibility was less than 2%.

Statistical analysis

The data were expressed as the mean±SD. The statistical analyses were conducted using the Student's paired *t*-test. The difference between the mean was considered statistically significant at $P<0.05$. The pharmacokinetic parameters were calculated with the Statistics software program DAS 2.0 (Mathematical Pharmacology Professional Committee of Shanghai, Shanghai, China). The statistical analysis of the standard curve was carried out by OriginPro 8.0 software (OriginLab Corporation, Northampton, USA).

Results

Optimization of preparation of nanoemulsion using central composite design response surface experiment

The three factors of the oil phase, surfactant to cosurfactant, and water phase were used as independent variables, and the particle size and encapsulation efficiency were considered as dependent variables; the nanoemulsion optimization was performed by the Design-Expert software. *F*-test and *P* value were used to analyze the statistical significance of the regression models, and the analysis of variance for the response surface models is shown in **Table 1**, and the multiple regression equations from the design expert software were as follows:

$$\begin{aligned} Y_1 &= 22.43 - 0.58A + 7.42B + 7.89C + 1.15AB - 3.37AC \\ &\quad - 6.93BC + 7.49A^2 + 5.31B^2 + 5.60C^2 (r = 0.9699, \\ &\quad P < 0.0001, \text{lack of fit} = 0.1383) \end{aligned}$$

$$\begin{aligned} Y_2 &= 93.23 + 5.72A + 6.08B + 4.72C + 0.04AB + 2.18AC \\ &\quad - 0.52BC - 22.79A^2 - 4.04B^2 - 1.86C^2 (r = 0.9711, \\ &\quad P < 0.0001, \text{Lack of fit} = 0.2197 \end{aligned}$$

The model of the regression equations of the particle size was significant with P value<0.05, P value of the lack of fit of the particle size was 0.1383, and the coefficient of R was fine. The predicted R^2 (0.8236) reasonably agreed with the adjusted R^2 (0.9420). The adequate precision was measured by the signal-to-noise ratio. A ratio greater than 4 was desirable. The ratio of 11.044 indicated an adequate signal. This model could be used to navigate the design space.

The model of the regression equations of the encapsulation efficiency was very significant with P value <0.0001, the P value of lack of fit of the encapsulation efficiency was 0.2197, and the coefficient of R was fine. The predicted R^2 of 0.8622 reasonably agreed with the adjusted R^2 of 0.9443. The ratio of adequate precision was 13.856, and this model was adequate.

According to the results of regression analysis, three-dimensional response surface diagrams of the relationship between independent variables and dependent variables were drawn (**Fig. 1**). Among the main factors affecting the particle size, the water phase (C) showed the greatest effect, followed by the surfactant and cosurfactant (B) and the interaction items (B and C). The particle size of nanoemulsion was increased with the S_{mix} and the water phase, and the effect of the oil phase (A) on the particle size was not

Table 1. Statistical analysis of variance for the central composite design response surface results

Source	Y_1				Y_2			
	Sum of squares	Mean square	*F* value	*P*	Sum of squares	Mean square	*F* value	*P*
Model	3443.87	382.65	17.62	<0.0001	5713.32	634.81	18.41	<0.0001
A-A	3.34	3.34	0.15	0.7030	325.31	325.31	9.43	0.0118
B-B	752.56	752.56	34.65	0.0002	505.28	505.28	14.65	0.0033
C-C	850.95	850.95	39.19	<0.0001	304.10	304.10	8.82	0.0141
AB	10.63	10.63	0.49	0.5002	0.015	0.015	<0.0001	0.9836
AC	90.72	90.72	4.18	0.0682	38.06	38.06	1.10	0.3182
BC	384.75	384.75	17.72	0.0018	2.13	2.13	0.062	0.8087
A^2	481.86	481.86	22.19	0.0008	4461.71	4461.71	129.38	<0.0001
B^2	408.60	408.60	18.82	0.0015	236.48	236.48	6.86	0.0257
C^2	455.31	455.31	20.97	0.0010	49.92	49.92	1.45	0.2566
Residual	217.16	21.72			344.85	34.48		
Lack of fit	160.60	32.12	2.84	0.1383	233.04	46.61	2.08	0.2197
Pure error	56.56	11.31			111.81	22.36		
Cor total	3661.03				6058.16			

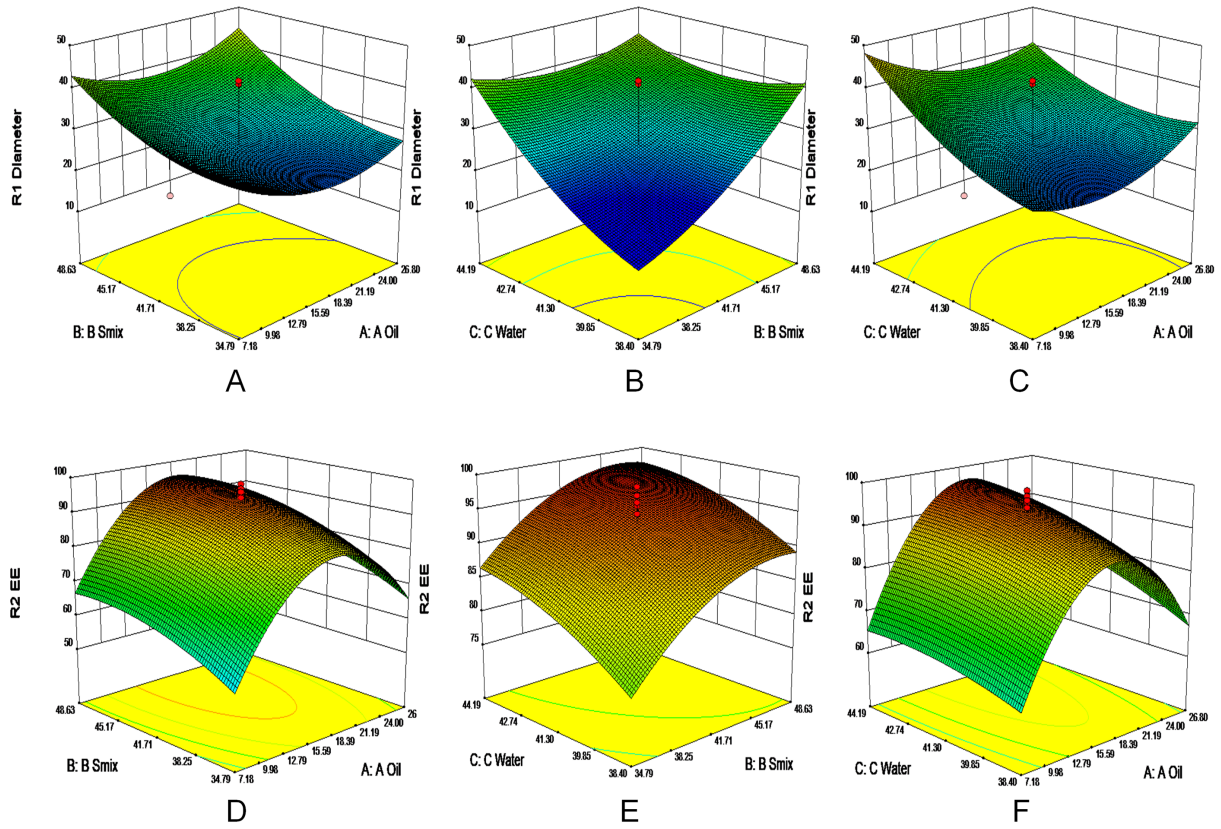

Figure 1. The response surface diagrams of particle size and encapsulation efficiency (A–C) The response surface diagrams of particle size (diameter). (D–F) The response surface diagrams of encapsulation efficiency (E).

very significant (**Fig. 1A—C**). As shown in **Fig. 1B**, the particle size was increased with the increasing values of the S_{mix} and water phase simultaneously, which implied that the interaction effects of B and C were positively significant. Among the main factors of the encapsulation efficiency, the quadratic of oil phase showed a significant effect, and other factors were not significant. Among the main factors affecting the encapsulation efficiency, the surfactant and cosurfactant showed the greatest effect, and the encapsulation efficiency of nanoemulsion was increased with the increase in the surfactant and cosurfactant (**Fig. 1D,E**). The oil phase and water phase also affected the encapsulation efficiency significantly (**Fig. 1D—F**). The encapsulation efficiency was increased first and then decreased with the increase in the oil phase, and the encapsulation efficiency was enhanced when the water phase was increased.

From the design response surface experiment, we evaluated the predictive optimum formulation composition of oil (16.5%), S_{mix} (38.7%), and water (44.8%). Three batches of samples were prepared in parallel according to the optimized conditions. The predicted and experimental values of the particle size were 23.72 nm and 23.16±0.25 nm, respectively, and the statistical prediction error was − 2.36%. The predicted and experimental values of the encapsulation efficiency were 93.67% and 98.15%±0.19%, respectively, and the statistical prediction error was 4.78%. The model fitted well with the actual situation.

Physiochemical characterization of nanoemulsion

Particle size and zeta potential are two important properties of nanoemulsion. Size of the droplets of buckwheat flavonoids nanoemulsion was 23.22±0.13 nm (**Fig. 2A**), PDI was 0.22±0.06, and zeta potential was − 20.92±0.27 mV (**Fig. 2B**), as determined using the dynamic light scattering method with a Malvern Zetasizer. **Fig. 2C** shows that the nanoemulsion appeared as a pale yellow clear liquid, and the morphology of the droplets was nearly spherical or spherical, as observed under the transmission electron microscope (**Fig. 2D**), and the particle size distribution was uniform. The encapsulation efficiency of the nanoemulsion was 98.35%±0.04%. After the storage at different temperatures for 30 days, the particle size and the zeta potential exhibited no significant change. No noticeable creaming was observed after centrifuging at 3000 *g* and 10,000 *g* for 10min.

Antioxidant activity study of nanoemulsion

The antioxidant capacity of buckwheat flavonoids nanoemulsion was assessed by DPPH scavenging activity, hydroxyl radical scavenging activity, and superoxide anion scavenging activity.

DPPH exhibits the maximum absorption at 517 nm owing to its stable nitrogen-containing free radicals, and its purple color turns yellow when the free radicals are scavenged by antioxidants. The antioxidant capacity of the nanoemulsion was evaluated and compared with that of the suspension using ascorbic acid as a positive control. As shown in **Fig. 3A**, the DPPH scavenging activity of nanoemulsion was increased with the concentration from 0.2 to 1.0 mg/ml, and the IC_{50} values of the nanoemulsion were 0.52 mg/ml. The DPPH radical scavenging activity curve of the suspension was also gradually increased, but at the concentration of 1.0 mg/ml, its scavenging activity was 37.1%, which was significantly lower than that of the nanoemulsion (81.92%). The results suggested that the nanoemulsion possessed potent DPPH free radical scavenging capacity.

Hydroxyl radicals are the most active free radicals, capable of lipid peroxidation and destruction of the biomacromolecules in cells. The buckwheat flavonoid nanoemulsion exhibited potent hydroxyl radical scavenging activity, and its activity was increased in a concentration-dependent manner (**Fig. 3B**). As a positive control, ascorbic acid displayed a strong free radical scavenging ability, and at the concentration of 1.0 mg/ml, the hydroxyl radical-scavenging activities of ascorbic acid, nanoemulsion, and suspension were 91.21%, 79.55%, and 40.45%, respectively. The scavenging ability of the nanoemulsion to hydroxyl radicals was significantly stronger than that of the suspension.

Pyrogallic acid is spontaneously oxidized under weak alkali conditions to form superoxide free radicals and intermediates, and its color varies with superoxide radical content. As shown in **Fig. 3C**, the superoxide anion scavenging ability of the nanoemulsion and suspension was increased in a concentration-dependent manner; at the concentration of 1.0 mg/ml, its maximum scavenging activity was 56.80%, which was obviously better than that of the nanoemulsion (29.15%). Compared with the DPPH and hydroxyl radicals scavenging abilities, superoxide anion scavenging abilities of nanoemulsion and suspension were significantly lower, indicating a moderate superoxide anion scavenging activity.

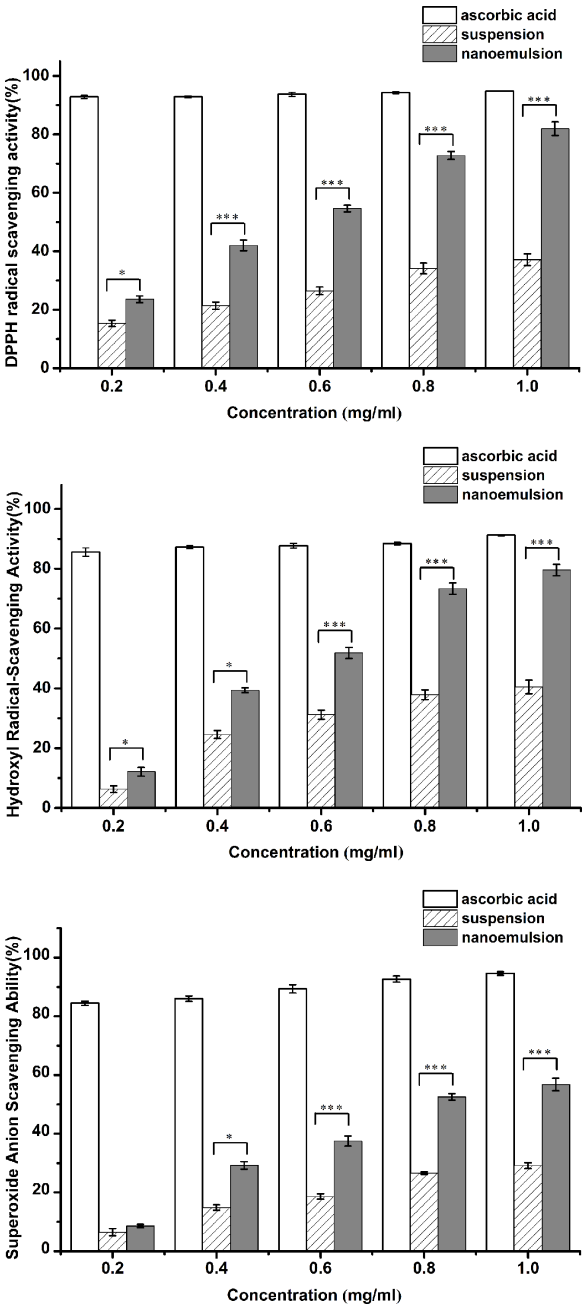

Figure 2. Characterization of nanoemulsion (A) Particle size and size distribution of nanoemulsion. (B) Zeta potential of nanoemulsion. (C) Appearance of nanoemulsion. (D) Transmission microscopy image of nanoemulsion with bar length 200 nm.

Cumulative release and model fitting of nanoemulsion

The *in vitro* release of the nanoemulsion was investigated using the dialysis method, and the drug release in the gastrointestinal tract

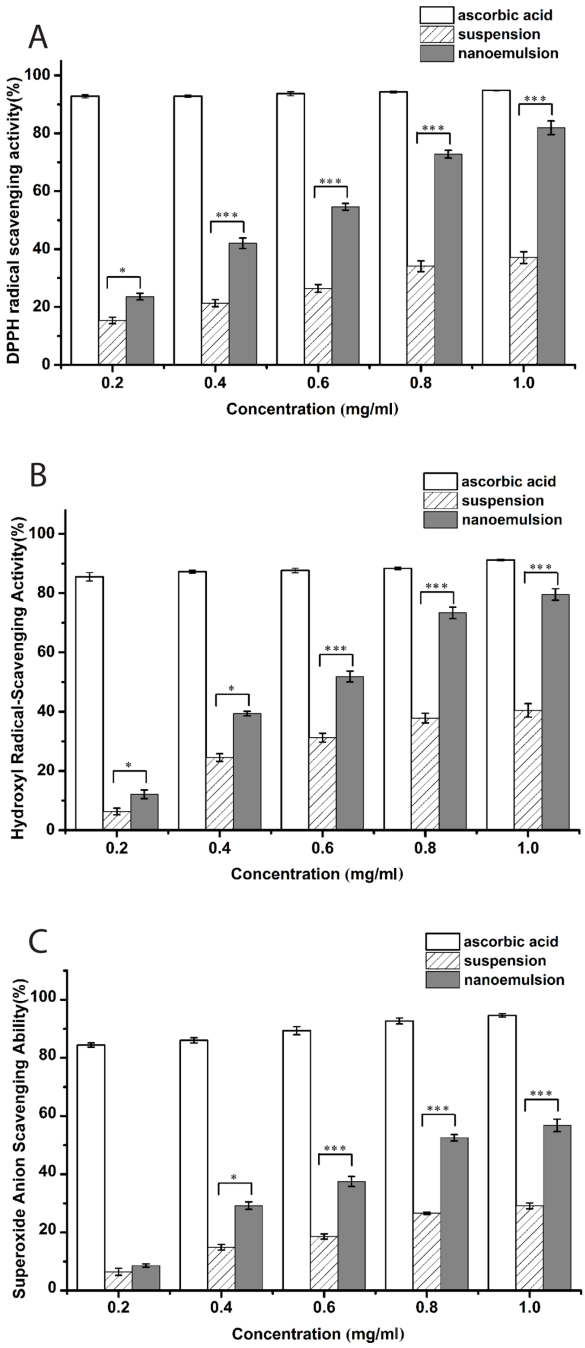

Figure 3. The antioxidant activities of the nanoemulsion and suspension The ascorbic acid was used as the positive control, and the nanoemulsion and suspension were the test samples. The statistical significance was analyzed by the Student's paired t-test with $P<0.05$ as the minimum level of significance, $P<0.01$ as the minimum level of very significance, and $P<0.001$ as the minimum level of extreme significance. (A) DPPH radical scavenging activity. (B) Hydroxyl radical scavenging activity. (C) Superoxide anion scavenging activity.

was simulated *in vitro*. A dialysis tube with a biofilm structure was placed in the buffer in a thermostatic bath at 37°C for simulating gastrointestinal fluid, and the drug digestion and peristalsis in the gastrointestinal tract were simulated by magnetic stirring.

The *in vitro* release of the buckwheat flavonoids nanoemulsion and suspension were continuously monitored for 48 h. The

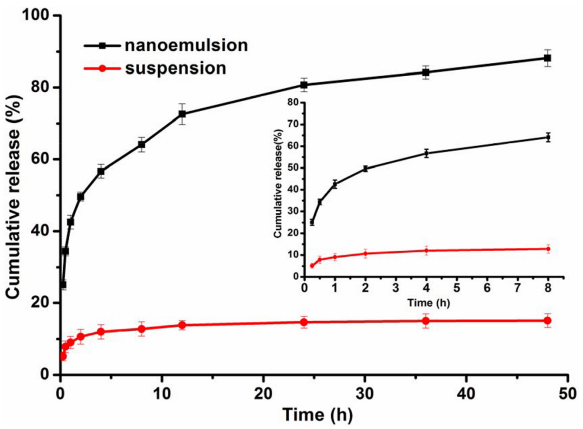

Figure 4. The cumulative release curves of the nanoemulsion and suspension The cumulative release curves was in 8 h and in 48 h through a dialysis membrane (molecular weight cutoff, MWCO, 8 kDa) at 37±0.5° C under stirring at 100 rpm.

cumulative release of the suspension was 5.17% in 15 min, and only 15.14% drug was released in 48 h because of its poor solubility (**Fig. 4**). The nanoemulsion released 25.09% in 15 min, 42.56% in 1 h, and the cumulative release was increased gradually until 88.16% of the drug was released in 48 h. The results showed that the cumulative release efficiency of the nanoemulsion was 5-folds higher than that of the suspension, and the effect of drugs *in vitro* was greatly improved.

Further studies on the release model fitting of the buckwheat flavonoids nanoemulsion were performed to understand the release pattern. Various dynamic models were fitted to the release curve, and the correlation coefficients (R^2), residual sum of squares (RSS), and Akaike information criterion (AIC) were calculated (**Table 2**). The drug release model was closer to Weibull ($R^2=0.9947$, RSS = 18.6194, AIC = 33.2369) and Ritger–Peppas ($R^2=0.9723$, RSS = 113.4027, AIC = 51.3095) models.

Pharmacokinetic parameters and bioavailability of nanoemulsion

The efficacy of the buckwheat flavonoids nanoemulsion was further verified by monitoring the buckwheat flavonoids plasma concentrations *in vivo* after intragastric administration to the test and control groups. The samples were analyzed by HPLC. The curves of the mean plasma concentration versus time for buckwheat flavonoids nanoemulsion and suspension are shown in **Fig. 5**. The pharmacokinetic parameters were calculated with the Statistics 2.0 software program (DAS 2.0), and the results are shown in **Table 3**.

In our study, the AUC for the nanoemulsion was 1621.2 ±141.60 ng/ml·h, which was 2.2-fold higher than that of the control suspension (734.48±109.81 ng/ml·h). The C_{max} (the maximum plasma drug concentration) of the nanoemulsion was 156.15±8.14 ng/ml, which was 2.6-fold higher than that of the suspension (59.89±6.49 ng/ml). The T_{max} (the maximum plasma drug concentration) of the nanoemulsion reached peak concentrations faster than the suspension within 0.90±0.22 h, which might be related to the good solubility of buckwheat flavonoids in the nanoemulsion. The nanoemulsion of buckwheat flavonoids exhibited significantly higher AUC than the suspension ($P<0.05$).

Table 2. Dynamic model fitting of the cumulative release curve and the correlation coefficients (R^2)

Model	Equation	R^2	RSS	AIC
Zero order	$Q = 1.1147\ t + 44.6680$	0.7441	1095.2628	73.9875
First order	$\ln(1 - 0.01Q) = -0.0359\ t + 4.0195$	0.9129	694.1201	69.4264
Higuchi	$Q = 9.0552\ t^{1/2} + 32.8700$	0.9062	401.4697	63.9513
Weibull	$\ln\ln[100/(100-Q)] = 0.3613 \ln t - 0.6594$	0.9947	18.6194	33.2369
Hixcon–Crowell	$(100 - Q)^{1/3} = -0.0368\ t + 3.8092$	0.8631	793.3247	70.7623
Ritger–Peppas	$\ln Q = 0.2246 \ln t + 3.6786$	0.9723	113.4027	51.3095

Notes: Q means cumulative release at time t.

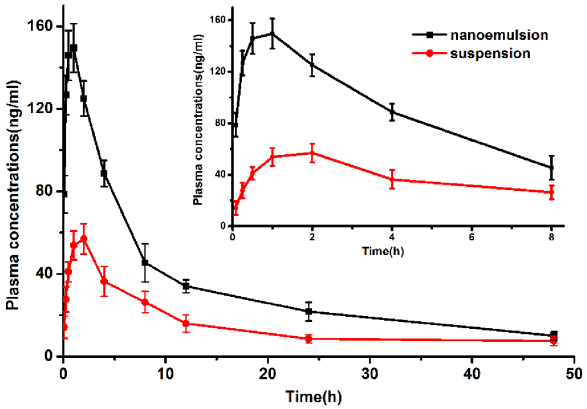

Figure 5. The plasma concentration-time curves of nanoemulsion and suspension The nanoemulsion and suspension were administered intragastrically to the Wistar rats (200±20 g) at a dose of 60 mg/kg. Data are shown as the mean±SD. On the right side, the plasma concentration-time curves of the first 8 h are displayed.

Table 3. The pharmacokinetic parameters of nanoemulsion and suspension in rats' plasma after intragastrical administration at a dose of 60 mg/kg

Parameter	Unit	Nanoemulsion	Suspension
AUC (0-t)	ng/ml·h	1621.26±141.60	734.48±109.81
AUC (0-∞)	ng/ml·h	1905.50±203.08	863.90±272.36
MRT (0-t)	h	13.16±0.98	14.90±1.47
MRT (0-∞)	h	22.68±3.74	26.26±8.55
t1/2z	h	19.66±3.26	14.60±8.31
T_{max}	h	0.90±0.22	1.60±0.55
C_{max}	ng/ml	156.15±8.14	59.89±6.49

Discussion

The CCD response surface experiment is a multivariate statistical method for optimization analysis [25], and it provides an idea of two more probability values, which can lead to a more comprehensive, intuitive, and accurate design. CCD was used in this study to determine the optimum conditions for nanoemulsion, which led to suitable particle size and encapsulation efficiency. The model effectively described and predicted the responses of the particle size and encapsulation efficiency with the changes in the constitution conditions in given experimental ranges. The particle size of nanoemulsion increased with the S_{mix} and water phase, and the effect of oil phase was not very significant. The surfactant and cosurfactant showed the greatest effects, and the oil phase and water phase also affected the encapsulation efficiency. The results of these experiments were close to the predicted values from the optimization analysis, suggesting that the multiple regression models are reasonable and reliable.

The nanoemulsion was obtained by the CCD experiment, and the nanoemulsion with small particle sizes displayed a smaller surface tension and greater stability. The smaller particle size can lead to a greater interfacial surface area for drug absorption, and the solubility and bioavailability are enhanced [26]. The zeta potential of the nanoemulsion is caused by the adsorption of charged molecules on its surface, which depends up on the types of emulsifier and the conditions of the medium, and this charge can cause molecular repulsions between dispersed phase droplets, so the zeta potential can improve the stability of the nanoemulsion [27–29]. In our study, buckwheat flavonoid nanoemulsion displayed a particle size within the abovementioned range, suggesting that our nanoemulsion system was stable.

Flavones possess antioxidant properties, but buckwheat flavonoid nanoemulsion showed significant antioxidant activity compared with suspensions in the three test methods because nanoemulsion technology can enhance the solubility and release of insoluble or poorly soluble drugs. A higher amount of drug might be responsible for the enhanced antioxidant potential [30]. The results of this study suggest that the SNEDDS is a feasible strategy to improve the antioxidant application, which can be potentially used as a natural antioxidant.

Drug release is the basis for all biological functions, including absorption, distribution, metabolism, and excretion. Drug release model fitting was performed to understand the release pattern [31]. As shown in **Table 2**, the best fitting parameters (R^2=0.9947, RSS=18.6194, AIC=33.2369) were derived from the Weibull model, and the *in vitro* drug release from the nanoemulsion followed this distribution, suggesting that the *in vitro* release process is continuous and dynamic, simulating the human digestive tract environment. It also indicated that the drug release has a sustained release trend. Ritger–Peppas (R^2=0.9723, RSS=113.4027, AIC=51.3095) might be similar to the drug released pattern, and its release mechanism might follow the Fickian diffusion (n<0.45) during the drug release process of the nanoemulsion. In our results, the *in vitro* release of the buckwheat flavonoids from the nanoemulsion was more advantageous than the suspension, which provided a potential possibility for the application of nanoemulsion flavonoids.

Bioavailability, an important criterion for evaluating the effect of drugs *in vivo*, is usually assessed by three parameters: C_{max}, T_{max}, and AUC. AUC is the most reliable indicator of bioavailability. It is directly proportional to the amount of prototype medicine that enters the body. This study demonstrated that the buckwheat flavonoid nanoemulsion is absorbed 2.2-fold higher than the suspension, as the drug particles in the nanoemulsion are relatively small and more drugs can be released. The absorption of a poorly water-soluble drug is often limited by its insufficient dissolution

in the gastrointestinal tract [32]. The small droplets of the drug-loaded nanoemulsion can pass through the membrane directly and get absorbed easily [33]. A self-nanoemulsifying drug delivery system of persimmon leaf extract was shown to accelerate the drug absorption, and the drug was not precipitated in the gastrointestinal tract [34]. Thus, the main problems of poor solubility and weak absorption of flavonoids were solved through the self-nanoemulsifying technology, and the oral bioavailability was significantly improved [35]. Nanoemulsion can be used as an effective carrier to improve the therapeutic effect of water-insoluble drugs.

In summary, this study was based on a previous experiment for developing buckwheat flavonoids into a nano-drug delivery system [36]. We constructed a drug delivery system and investigated its characteristics *in vitro* and the drug delivery to animals *in vivo*, which provided a theoretical basis for the application of buckwheat flavonoids in clinical practice. Our results demonstrated that nanoemulsion is an effective drug delivery system that can significantly improve the antioxidant activity, *in vitro* release, and bioavailability compared with the corresponding drug suspension. Nanoemulsion can improve the oral absorption of drugs, promote the dissolution of the poorly soluble drugs, and enhance the bioavailability of drugs.

Funding

This work was supported by the grants from the Applied Basic Research Programs of Shanxi Province (No. 201801D121192) and the Scientific and Technological Innovation Programs of Higher Education Institutions in Shanxi Province (No. 201802020).

References

1. Ahmed A, Khalid N, Ahmad A, Abbasi NA, Latif MSZ, Randhawa MA. Phytochemicals and biofunctional properties of buckwheat: a review. *J Agric Sci* 2013, 152: 349–369.
2. Xu QL, Wang L, Li WX, Xing YG, Zhang P, Wang Q, Li H, *et al*. Scented tartary buckwheat tea: aroma components and antioxidant activity. *Molecules* 2019, 24: 4368.
3. Zhou XL, Chen ZD, Zhou YM, Shi RH, Li ZJ. The effect of tartary buckwheat flavonoids in inhibiting the proliferation of MGC80-3 cells during seed germination. *Molecules* 2019, 24: 3092.
4. Jing R, Li HQ, Hu CL, Jiang YP, Qin LP, Zheng CJ. Phytochemical and pharmacological profiles of three Fagopyrum buckwheats. *Int J Mol Sci* 2016, 17: 589.
5. Mustapha O, Kim KS, Shafique S, Kim DS, Jin SG, Seo YG, Youn YS, *et al*. Development of novel cilostazol-loaded solid SNEDDS using a SPG membrane emulsification technique: physicochemical characterization and *in vivo* evaluation. *Colloids Surf, B* 2017, 150: 216–222.
6. Singh G, Pai RS. Trans-resveratrol self-nano-emulsifying drug delivery system (SNEDDS) with enhanced bioavailability potential: optimization, pharmacokinetics and in situ single pass intestinal perfusion (SPIP) studies. *Drug Deliv* 2015, 22: 522–530.
7. Syukri Y, Martien R, Lukitaningsih E, Nugroho AE. Novel self-nano emulsifying drug delivery system (SNEDDS) of andrographolide isolated from Andrographis paniculata nees: characterization, in-vitro and in-vivo assessment. *J Drug Delivery Sci* 2018, 47: 514–520.
8. Kumar M, Bishnoi RS, Shukla AK, Jain CP. Techniques for formulation of nanoemulsion drug delivery system: a review. *Prev Nutr Food Sci* 2019, 24: 225–234.
9. Singh Y, Meher JG, Raval K, Khan FA, Chaurasia M, Jain NK, Chourasia MK. Nanoemulsion: concepts, development and applications in drug delivery. *J Controll Release* 2017, 252: 28–49.
10. Gurram AK, Deshpande PB, Kar SS, Nayak UY, Udupa N, Reddy MS. Role of components in the formation of self-microemulsifying drug delivery systems. *Indian J Pharm Sci* 2015, 77: 249–257.
11. Sole I, Solans C, Maestro A, Gonzalez C, Gutierrez JM. Study of nano-emulsion formation by dilution of microemulsions. *J Colloid Interface Sci* 2012, 376: 133–139.
12. Solans C, Solé I. Nano-emulsions: formation by low-energy methods. *Curr Opin Colloid Interface Sci* 2012, 17: 246–254.
13. Chen Y, Zhang HY, Yang J, Sun HY. Improved antioxidant capacity of optimization of a self-microemulsifying drug delivery system for resveratrol. *Molecules* 2015, 20: 21167–21177.
14. Liu HF, Mei JA, Xu Y, Tang L, Chen DQ, Zhu YT, Huang SG, *et al*. Improving the oral absorption of Nintedanib by a self-microemulsion drug delivery system: preparation and in vitro/in vivo evaluation. *Int J Nanomed* 2019, 14: 8739–8751.
15. Liang XL, Chen XL, Zhao GW, Tang T, Dong W, Wang CY, Zhang J, *et al*. Preparation, characterization, and pharmacokinetic evaluation of imperatorin lipid microspheres and their effect on the proliferation of MDA-MB-231 cells. *Pharmaceutics* 2018, 10: 236.
16. Kotta S, Khan AW, Ansari SH, Sharma RK, Ali J. Formulation of nanoemulsion: a comparison between phase inversion composition method and high-pressure homogenization method. *Drug Deliv* 2015, 22: 455–466.
17. Wang W, Bostic TR, Gu LW. Antioxidant capacities, procyanidins and pigments in avocados of different strains and cultivars. *Food Chem* 2010, 122: 1193–1198.
18. Sabeena Farvin KH, Andersen LL, Otte J, Nielsen HH, Jessen F, Jacobsen C. Antioxidant activity of cod (Gadus morhua) protein hydrolysates: fractionation and characterisation of peptide fractions. *Food Chem* 2016, 204: 409–419.
19. Brizzolari A, Campisi GM, Santaniello E, Razzaghi-Asl N, Saso L, Foti MC. Effect of organic co-solvents in the evaluation of the hydroxyl radical scavenging activity by the 2-deoxyribose degradation assay: the paradigmatic case of alpha-lipoic acid. *Biophys Chem* 2017, 220: 1–6.
20. Zou SQ, Zhu XF, Zhang LR, Guo F, Zhang MM, Tan YW, Gong AH, *et al*. Biomineralization-inspired synthesis of cerium-doped carbonaceous nanoparticles for highly hydroxyl radical scavenging activity. *Nanoscale Res Lett* 2018, 13: 76.
21. Subhaswaraj P, Sowmya M, Jobina R, Sudharshan SJ, Dyavaiah M, Siddhardha B. Determination of antioxidant potential of Acacia nilotica leaf extract in oxidative stress response system of saccharomyces cerevisiae. *J Sci Food Agric* 2017, 97: 5247–5253.
22. Wang LL, Huang S, Guo HH, Han YX, Zheng WS, Jiang JD. In situ delivery of thermosensitive gel-mediated 5-fluorouracil microemulsion for the treatment of colorectal cancer. *Drug Des, Dev Ther* 2016, 10: 2855–2867.
23. Tsai YM, Jan WC, Chien CF, Lee WC, Lin LC, Tsai TH. Optimised nano-formulation on the bioavailability of hydrophobic polyphenol, curcumin, in freely-moving rats. *Food Chem* 2011, 127: 918–925.
24. Alhakamy NA, Fahmy UA, Ahmed OAA. Attenuation of benign prostatic hyperplasia by optimized Tadalafil loaded pumpkin seed oil-based self nanoemulsion: in vitro and in vivo evaluation. *Pharmaceutics* 2019, 11: 640.
25. Ahmad N, Ahmad FJ, Bedi S, Sharma S, Umar S, Ansari MA. A novel nanoformulation development of eugenol and their treatment in inflammation and periodontitis. *Society Saudi Pharm J* 2019, 27: 778–790.
26. Ferreira LM, Sari MHM, Cervi VF, Gehrcke M, Barbieri AV, Zborowski VA, Beck RCR, *et al*. Pomegranate seed oil nanoemulsions improve the photostability and in vivo antinociceptive effect of a non-steroidal anti-inflammatory drug. *Colloids Surf, B* 2016, 144: 214–221.
27. Lago AMT, Neves ICO, Oliveira NL, Botrel DA, Minim LA, de Resende JV. Ultrasound-assisted oil-in-water nanoemulsion produced from Pereskia aculeata Miller mucilage. *Ultrason Sonochem* 2019, 50: 339–353.
28. Mohammadzadeh H, Koocheki A, Kadkhodaee R, Razavi SMA. Physical and flow properties of d-limonene-in-water emulsions stabilized with

whey protein concentrate and wild sage (Salvia macrosiphon) seed gum. *Food Res Int* 2013, 53: 312–318.
29. Shanmugam A, Ashokkumar M. Ultrasonic preparation of stable flax seed oil emulsions in dairy systems – physicochemical characterization. *Food Hydrocoll* 2014, 39: 151–162.
30. Balasubramani S, Rajendhiran T, Moola AK, Diana RKB. Development of nanoemulsion from Vitex negundo L. essential oil and their efficacy of antioxidant, antimicrobial and larvicidal activities (Aedes aegypti L.). *Environ Sci Pollut Res* 2017, 24: 15125–15133.
31. Jain A, Jain SK. In vitro release kinetics model fitting of liposomes: an insight. *Chem Phys Lipids* 2016, 201: 28–40.
32. Zhang P, Liu Y, Feng NP, Xu J. Preparation and evaluation of self-microemulsifying drug delivery system of oridonin. *Int J Pharm* 2008, 355: 269–276.
33. De Smidt PC, Campanero MA, Troconiz IF. Intestinal absorption of penclomedine from lipid vehicles in the conscious rat: contribution of emulsification versus digestibility. *Int J Pharm* 2004, 270: 109–118.
34. Li WW, Yi SL, Wang ZH, Chen S, Xin S, Xie JW, Zhao CS. Self-nanoemulsifying drug delivery system of persimmon leaf extract: optimization and bioavailability studies. *Int J Pharm* 2011, 420: 161–171.
35. Wan K, Sun LL, Hu XY, Yan ZJ, Zhang YH, Zhang X, Zhang JQ. Novel nanoemulsion based lipid nanosystems for favorable in vitro and in vivo characteristics of curcumin. *Int J Pharm* 2016, 504: 80–88.
36. Cui XD, Wang ZH. Preparation and properties of rutin-hydrolyzing enzyme from tartary buckwheat seeds. *Food Chem* 2012, 132: 60–66.